The effect of spatial averaging and glacier melt on detecting a forced signal in regional sea level

2017 Environ. Res. Lett. 12 034004

(http://iopscience.iop.org/1748-9326/12/3/034004)

Environmental Research Letters

LETTER

The effect of spatial averaging and glacier melt on detecting a forced signal in regional sea level

Kristin Richter[1,4], Ben Marzeion[2] and Riccardo Riva[3]

[1] Institute for Atmospheric and Cryospheric Sciences, University of Innsbruck, Innrain 52f, 6020 Innsbruck, Austria
[2] Institute of Geography, University of Bremen, Bremen, Germany
[3] Faculty of Civil Engineering and Geosciences, Delft University of Technology, Netherlands
[4] Author to whom any correspondence should be addressed.

E-mail: kristin.richter@uibk.ac.at

Keywords: regional sea level, internal variability, time of emergence, detection

Supplementary material for this article is available online

OPEN ACCESS

RECEIVED
8 November 2016

REVISED
2 January 2017

ACCEPTED FOR PUBLICATION
13 January 2017

PUBLISHED
27 February 2017

Abstract

We investigate the spatial scales that are necessary to detect an externally forced signal in regional sea level within a selected fixed time period. Detection on a regional scale is challenging due to the increasing magnitude of unforced variability in dynamic sea level on progressingly smaller spatial scales. Using unforced control simulations with no evolving forcing we quantify the magnitude of regional internal variability depending on the degree of spatial averaging. We test various averaging techniques such as zonal averaging and averaging grid points within selected radii. By comparing the results from the control simulations with historical and 21st-century simulations, the procedure allows to estimate to what degree the data has to be averaged spatially in order to detect a forced signal within certain periods (e.g. periods with good observational coverage).

We find that zonal averaging over ocean basins is necessary to detect a forced signal in steric and dynamic sea level during the past 25 years, while a signal emerges in 63% of the ocean areas over the past 45 years when smoothing with a 2000 km filter or less is applied. We also demonstrate that the addition of the glacier contribution increases the signal-to-noise ratio of regional sea level changes, thus leading to an earlier emergence by 10–20 years away from the sources of the ice mass loss. With smoothing, this results in the detection of an external signal in 90% of the ocean areas over the past 45 years.

1. Introduction

Through anthropogenic emissions the radiative balance of the Earth system is significantly altered (Myhre *et al* 2013). This so-called anthropogenic forcing results in an adjustment of the climate system expressed in changes of key variables such as the increase of global mean surface temperature and sea level. However, due to inherent natural climate variability, it is not straightforward to distinguish the forced anthropogenic signal from the background noise, let alone to quantify it. With respect to sea level, various detection and attribution studies have found an anthropogenically forced signal in global thermosteric sea surface height (Marcos and Amores 2014, Slangen *et al* 2014b), in glacier mass contribution (Marzeion *et al* 2014b) as well as total global sea level rise (Dangendorf *et al* 2015, Slangen *et al* 2016).

Detection on regional to local scales is complicated by the increased magnitude of internal variability that can easily offset a forced signal on smaller spatial scales (Marcos and Amores 2014). Recent studies attempted to quantify local internal variability by using unforced control simulations of CMIP5 climate models (Meyssignac *et al* 2012, Lyu *et al* 2014, Richter and Marzeion 2014) or statistical models (Dangendorf *et al* 2015). Those studies also assessed the time of emergence of an externally forced signal in steric and dynamic sea surface height in climate simulations. They found that, in regions of elevated internal variability such as the western tropical Pacific Ocean, it can take several decades for a forced signal to emerge

from the background noise. Lyu *et al* (2014) also showed that the land ice contribution potentially reduces the time of emergence by several decades in selected regions. In addition, the emergence of an externally forced signal did not only depend on the location but also on the time periods considered.

Global coverage of sea level through satellite altimetry is available starting in 1992, i.e. for less than 25 years. Data coverage from upper ocean observations of temperature and salinity only starts to be reasonably sufficient to compute changes in ocean heat content and steric height changes on a regional scale after 1970 (Domingues *et al* 2008, e.g.). Are these periods long enough for an externally forced signal to emerge from the noise of internal variability on a regional scale? According to Richter and Marzeion (2014), starting from 1970 the regional emergence of a signal in steric and dynamic sea surface height will take more than 50 years in more than 87% of the worldwide ocean area. Thus, it will not be detected by now without accounting for internal variability.

To detect an externally forced signal in sea level on scales smaller than the global, regional averaging will be necessary to increase the signal to noise ratio. In this study we will investigate how spatial averaging reduces the noise and whether this will allow for an earlier detection compared to earlier studies where no spatial averaging was performed. By identifying, for each location, the averaging method that is necessary to detect an external signal during a selected time period, it can be assessed on which spatial scales regional detection and attribution studies may yield meaningful results. More specifically, we will determine how much we need to average spatially to detect an externally forced signal in two selected time periods, namely 1970–2015 and 1990–2015, the approximate periods of reliable observations from hydrography (and therefore steric height) and satellite altimetry, respectively. We will also consider glacier melt and will investigate in more detail how it affects the time of emergence on regional scales.

2. Data and methods

In this study, we use output from climate models that participated in the Coupled Model Intercomparison Project Phase 5 (CMIP5, Taylor *et al* (2012)). The sea surface height above the geoid is combined with the global mean thermosteric height change to yield the regional steric height change including dynamic effects. The data was averaged to annual resolution. The fields were drift-corrected by removing the linear trend found in the unforced control simulations from the scenario simulations. With one exception, the control simulations cover at least 500 yrs (table S1 stacks.iop.org/ERL/12/034004/mmedia). The scenario simulations comprise the historical simulations that typically cover the period 1850–2005 as well as the RCP4.5 scenario (2006–2100), a scenario with moderate reductions in greenhouse gas emissions (Van Vuuren *et al* 2011). The processed data is remapped to a regular grid of $1 \times 1^{\circ}$ resolution.

Surface temperature and precipitation fields from the same models and simulations are used to force a global glacier model described in detail by Marzeion *et al* (2012) and Marzeion *et al* (2014a). The model computes the annual specific mass balance for each of the worlds individual glaciers in the Randolph Glacier Inventory v4.0 (Arendt *et al* 2015) and aggregates the results into 18 regions. It does not model glacier dynamics explicitly but allows for changes in the glacier hypsometry (volume, surface area and elevation range). Antarctic peripheral glaciers are excluded, as there are not enough observations to calibrate the model in this region. The model has been successfully used in sea level budget studies (Gregory *et al* 2013), impact studies (Marzeion and Levermann 2014, Hinkel *et al* 2014) as well as detection and attribution studies (Marzeion *et al* 2014b). To translate the glacier model output into regional sea level changes, the mass changes for the 18 regions are multiplied by the normalized gravitational fingerprints for each region. The individual fingerprints have been obtained by assuming the melt of a uniform ice layer over the glaciated area in each region and by computing the induced sea level change after solving the sea level equation (Farrell and Clark 1976), including the rotational feedback (Milne and Mitrovica 1998), on a compressible elastic earth (Dziewonski and Anderson 1981).

The final dataset consists of 12 models with concurrent data output from the glacier model and steric and dynamic height from CMIP5 models (table S1). We then follow the procedure by Richter and Marzeion (2014). The control simulations are used to estimate the magnitude of unforced variability: multi-pentadal sliding windows of a length from 10 to 100 years are used to quantify the range of unforced linear trends on the time scales defined by the window length. By comparing these trends with trends found in the historical and future simulations, the time of emergence of a forced trend, i.e. a trend not consistent with the trends found in the control simulations, is identified (see figure S1 for an illustration of the procedure). The procedure is repeated after subjecting the original data to various spatial averaging techniques, namely zonal averaging over all longitudes, zonal averaging over the individual ocean basins (Atlantic, Pacific and Indian Ocean) as well as averaging all data within a selected radius (500, 1000, 1500 and 2000 km). We perform the analysis on steric height only, as well as on the combined contributions of steric height and glacier mass loss. Also, the analysis is carried out for each model individually but for clarity, results are presented for the ensemble mean only. As mentioned in the introduction, we focus on the two approximate periods with sufficient global coverage of observations, namely 1970–2015 and 1990–2015.

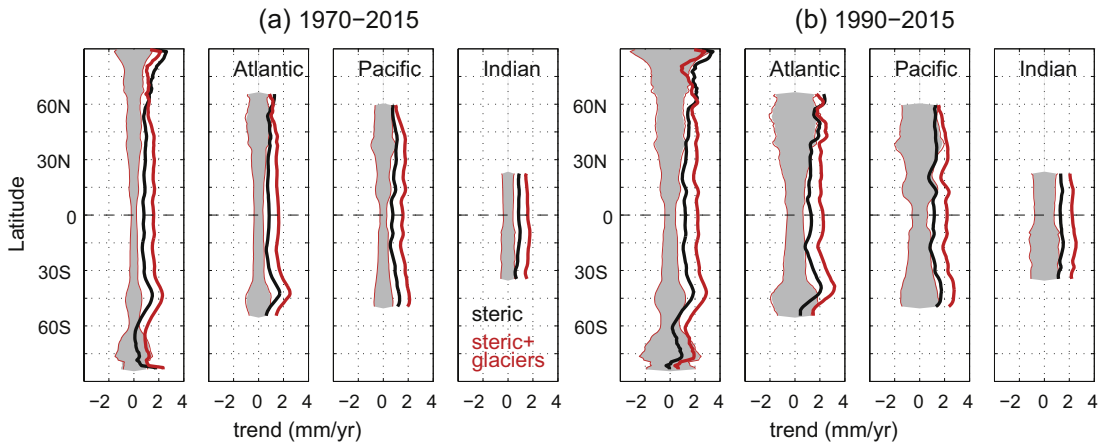

Figure 1. Linear trends in dynamic sea level (thick black line) and dynamic sea level+glaciers (red line) from zonally averaged data. The gray envelope encloses the 5th–95th percentile of dynamic sea level linear trends from the control simulations while the thin red line includes the glacier mass loss contribution. Multi-model mean is shown for the two periods (*a*) past 45 years (1970–2015) and (*b*) past 25 years (1990–2015)

3. Results

3.1. Zonal averages

To illustrate our method, we present linear trends of zonally averaged sea surface height for the two periods (1970–2015 and 1990–2015) and compare them to internal variability (figure 1). We start by examining the magnitude of internal variability shown as gray envelope on a 45-yr and 25-yr time scale in figure 1(*a*) and (*b*), respectively. As mentioned, the ensemble mean variability is presented and the magnitude in individual models might be larger or smaller. As expected, unforced linear trends are larger on shorter time scales (see also figure S2). On both time scales, there is elevated internal variability at the poles and a minimum at the equator. In the Pacific Ocean, ENSO-related dynamics lead to a local maximum in internal variability in the northern tropics at around 15 °N, while the signature of the western boundary current (Kuroshio Current) is evident at around 40 °N on both time scales (though more pronounced on the shorter period, figure 1*b*). In the North Atlantic Ocean, the signature of the western boundary current (Gulf Stream) is less localized and characterized by a broader maximum in internal variability centered around 50 °N (compare also with figure 3(*a*) and (*b*)). Apart from the polar regions, absolute unforced linear trends do not exceed 1 mm yr^{-1} (2 mm yr^{-1}) on a 45-yr (25-yr) time scale. The contribution of glacier mass change to variability in zonally averaged sea surface height is negligible.

We will now compare the trends induced by internal variability as discussed above with ensemble mean modeled trends from the historical simulations (thick lines in figure 1). Modeled historical trends are larger for 1990–2015 as compared to 1970–2015. With the exception of the Southern Ocean (south of 60 °S), linear trends of the zonally averaged steric sea level are outside the range of internal variability for both periods when averaging over all longitudes. The meridional variability of the linear trends is larger for the shorter period. When looking at single basins, historical trends in steric height are closer to the upper bound of what could be explained with unforced variability or, in case of the 25-yr period, partly within the envelope of internal variability, particularly at mid-latitudes. A striking feature is the local maximum in the mid-latitudes of the South Atlantic Ocean just north of 45 °S that is located slightly north of the local maximum in internal variability. In contrast, a local minimum is present in the North Atlantic just south of 60 °N. However, it is located inside the range of internal variability.

When the glacier mass loss contribution is taken into account (thick red lines in figure 1), trends are generally larger and well outside the noise range except in the Arctic and Southern Oceans. South of around 50 °N the glacier contribution leads to a zonally uniform increase in modeled trends of ≈ 0.8 mm yr^{-1} (1970–2015) and 1.0 mm yr^{-1} (1990–2015), respectively. This is due to the gravitational adjustment of the sea surface following the loss of mass (through glacier retreat on the surrounding land) and therefore gravitational attraction. Since most of the glaciers are situated in the Arctic (as we do not consider Antarctic glaciers), the effect is largest there and the contributions from glacier mass loss reduce modeled trends north of 60 °N.

From figure 1 it can be seen that simulated linear trends in zonally averaged steric and glacier loss sea surface height in both periods are partly forced, i.e. outside the noise range. To assess how the period needed for an external signal to emerge from the noise, and therefore also the time of emergence, depends on the start year, we compute the time of emergence for all start years between 1960–1995 (figure 2). This will reveal whether a forced trend can also be detected in a period shorter than 25 yrs (the shortest period we test

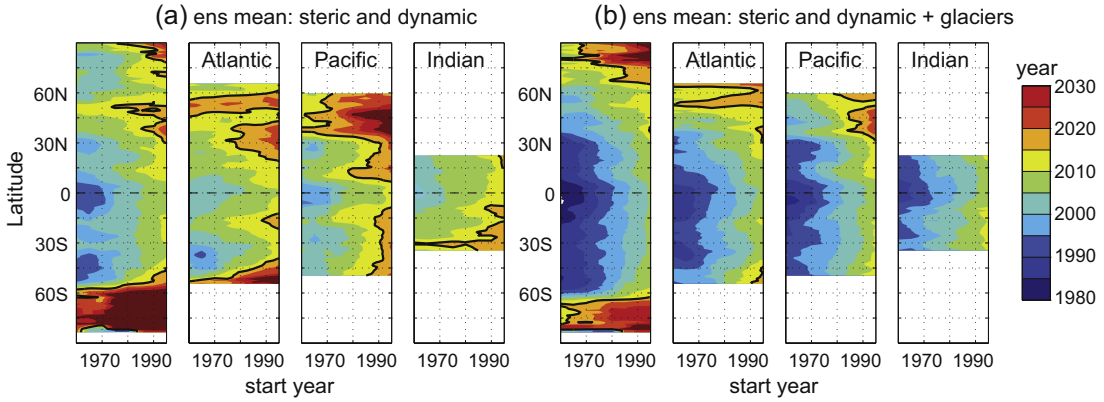

Figure 2. Ensemble mean time of emergence of an external signal as a function of start year for zonally averaged data. The data has been averaged over all longitudes, as well as the single ocean basins. The black line represents emergence in 2015.

is 10 yrs) or if detection in the Southern Ocean is possible by using longer periods (i.e. by starting before 1970).

With respect to steric height (figure 2(*a*)), enhanced noise leads to a delayed detection in the mid-latitudes of the Northern hemisphere compared to the tropics and mid-latitudes of the Southern hemisphere. This is most pronounced in the North Atlantic and North Pacific Ocean. In general, the later the start year the later a forced signal emerges. However, the actual time span it takes for a forced signal to emerge from the noise decreases with the start year, implying an acceleration (figure S3, lower row) of the forced signal. The exception are the polar regions and the northern mid-latitudes of the Atlantic Ocean where the timing appears to be independent of the start year (figure 2). No external signal is detectable in the Northern Pacific when starting later than 1970. Away from the polar regions and the northern Pacific Ocean, detection is possible in less than 30–40 yrs when starting in 1995 and even in 20 yrs at the equator in all basins and between 30–40 °S in the Atlantic Ocean.

When the glacier mass contribution is added, an external signal emerges much earlier (figure 2(*b*)) which is due to the high signal-to-noise ratio of this contribution. Also here, the exception is the Arctic Ocean and the northern North Atlantic for reasons mentioned earlier. Detection in the Arctic Ocean is only possible for long periods and not at all in the Southern Ocean. For the remaining area, an externally forced signal is detectable well before 2015, even when starting in the 1990s.

3.2. Spatial smoothing

Figures 1 and 2 suggest that, in some regions, it is possible to go to higher spatial resolution than zonal averages to detect an externally forced signal within the considered observational periods. We therefore smoothed the data by averaging over all grid points within four selected radii (500, 1000, 1500, 2000 km, respectively) and repeated our analysis (see figure 3(*f*) and (*i*) for an impression of the range of the smoothing). We expect a reduction in internal variability due to the spatial smoothing.

Indeed, figure 3 shows weaker internal variability on all time scales after smoothing the data prior to quantifying internal variability. Without smoothing, the main features are relatively small variability in the tropical oceans and enhanced variability in the western boundary currents on all time scales (see Richter and Marzeion (2014) for a more thorough discussion of the internal variability). These features are still present but strongly reduced in magnitude after smoothing with a 1000 km radius. Going to 2000 km, the patterns are no longer distinct. The effect of spatial smoothing is not equivalent to considering longer time scales. At 60 yrs and no smoothing the typical features are still discernible, although largely reduced in magnitude. Spatial smoothing on those multi-decadal time scales has a smaller effect and smoothing beyond 1000 km is futile. Adding the glacier mass change contribution makes only a negligible difference across most of the oceans area (not shown).

We will now investigate how spatial smoothing affects the time of emergence. Again, considering the advent of good observational coverage, we choose to look at two different start years, namely 1970 and 1990 (figure 4). In accordance with figure 2, the time of emergence is earlier when linear trends are computed for a period starting in 1970 compared to 1990. With the exception of the high Arctic region, including glacier mass loss shifts the emergence to an earlier point in time by about 10–20 yr in most of the Pacific and parts of the Atlantic and Indian Oceans (figure 5). While, for example, a forced signal in steric height emerges only in the tropical Atlantic by 2015, detection is possible in large parts of the mid-latitude Atlantic and the eastern Pacific Ocean by then, when glacier mass loss is included (compare figure 4(*a*) and (*b*)). Starting in 1990, virtually no signal that is distinct from noise emerges in steric height by 2015 and even when glaciers are included, a signal emerges in the tropical Atlantic and in some parts of the other tropical basins only (figure 4(*c*) and (*d*)).

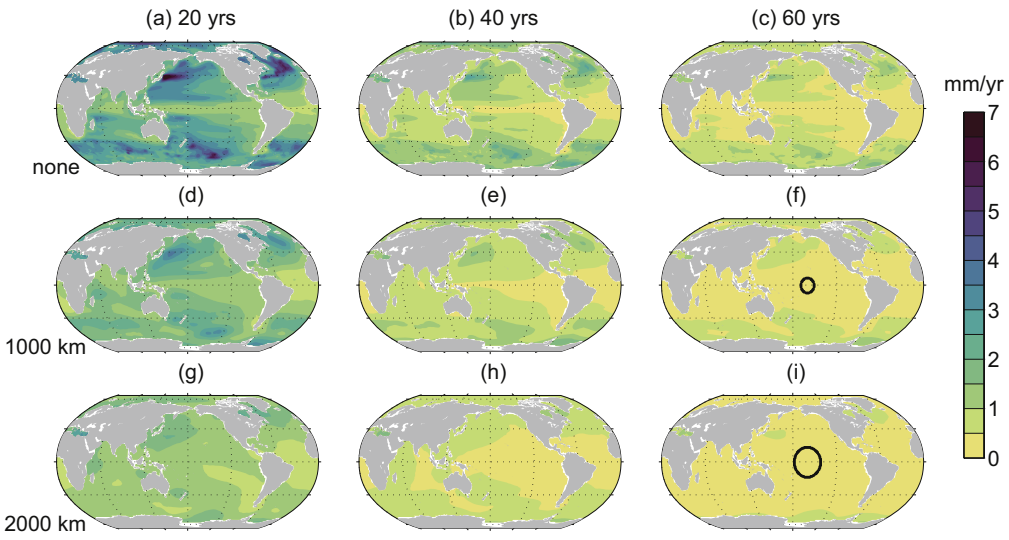

Figure 3. Magnitude of upper trends (in mm yr^{-1}) in regional steric height due to internal variability for selected time periods of 20 (left), 40 (middle) and 60 yrs (right). The upper row shows the trends without prior spatial smoothing, the data has been smoothed using a 1000 km radius and a 2000 km radius in the second and third row, respectively. The circles in panels (*f*) and (*i*) represent areas with a 1000 and 2000 km radius, respectively.

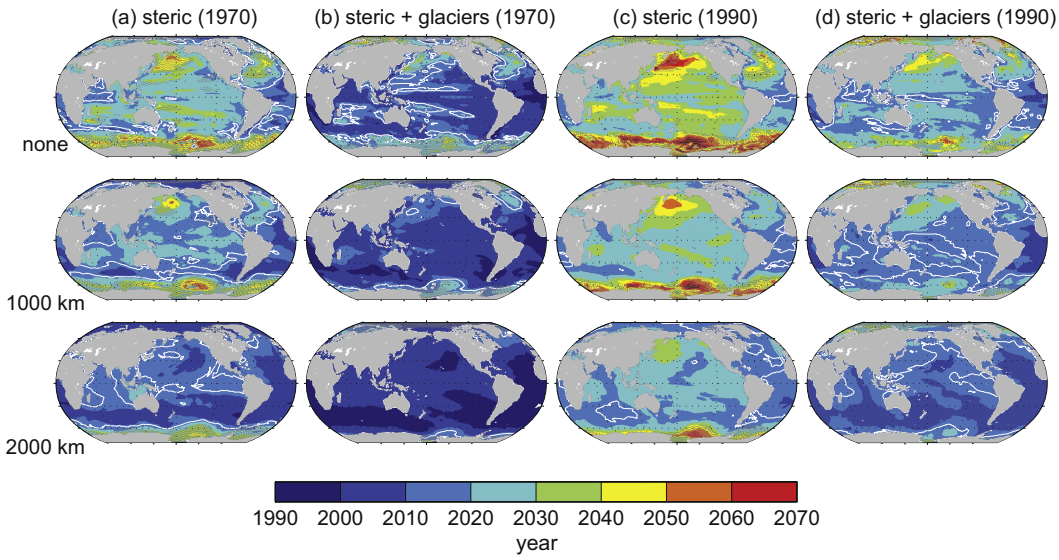

Figure 4. Time of emergence of a forced signal in regional steric height (*a*+*c*) and the combination with glacier mass loss (*b*+*d*) for the start year 1970 (*a*+*b*) and 1990 (*c*+*d*), respectively. The rows show the dependence of the time of emergence on the grade of smoothing. The hatched areas present regions where not all models show a forced signal emerge within a 100 yrs, i.e. the time of emergence in these areas is biased low. The white line represents emergence in 2015.

With respect to the polar regions, the inclusion of glaciers enhances the chances of detection in the Southern Ocean (no Antarctic glaciers). In contrast, in the Arctic Ocean and Nordic Seas, the detection of an external signal is delayed except for a narrow region around the heavily glaciated islands of Svalbard and Franz Josef Land (figure 5(*c*)). This is due to a partial canceling of the positive effect of thermal expansion and the negative effect of gravitational adjustment due to glacier mass loss leading to a small signal that is overwhelmed by noise. Close to Svalbard and Franz Josef Land the glacier mass loss signal dominates, resulting in a strong sea level drop that is distinct from the noise. It should however be noticed that the ensemble standard deviation is as strong as the ensemble mean signal and this result needs to be treated with caution (figure 5).

When spatial smoothing is applied, the time it takes for a forced signal to emerge is generally reduced. For example, smoothing regional sea surface height from steric and glacier mass changes with a 1000 km filter leads to a detection of an external signal before 2015 in 74% of the ocean areas when starting in 1970 (figure 4(*b*) and table 1). Even when starting in 1990, the glacier mass loss contribution to sea surface height changes enhances the signal-to-noise ratio in such a way that, with strong smoothing, detection is possible in up to 61% (figure 4(*d*), lower row). The exceptions

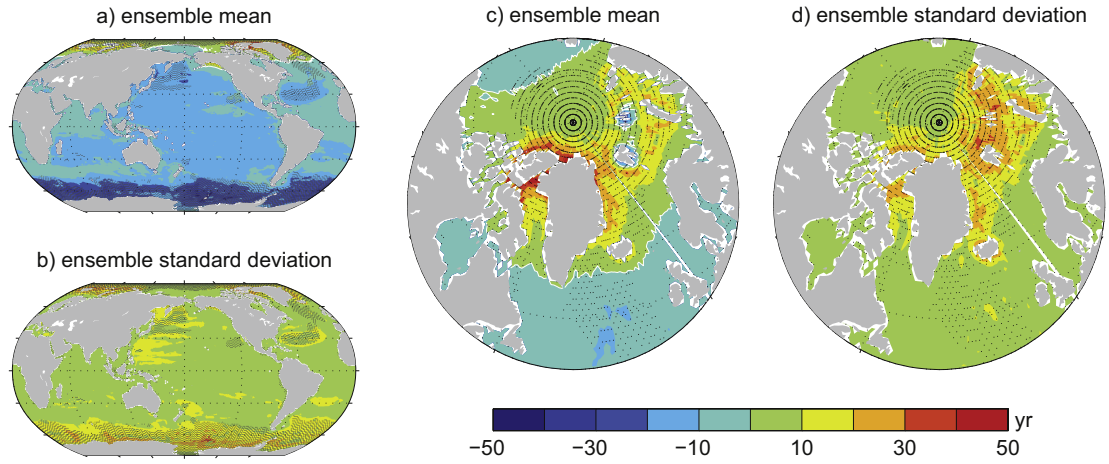

Figure 5. *a+c*) Ensemble mean and *b+d*) standard deviation of change in time of emergence when glacier mass loss is taken into account (negative values correspond to earlier emergence). The start year is 1990, but results are very similar for start year of 1970. Panel *c+d* zoom in on Arctic and northern North Atlantic Ocean. The hatched area presents regions where not all models show a forced signal emerge in either steric height only or steric height in combination with glacier mass loss.

Table 1. Multi-model mean fraction of ocean area (in %) with detection before or in 2015.

filter	steric 1970	steric+glac 1970	steric 1990	steric+glac 1990
none	13	54	1	10
1000 km	31	74	3	25
2000 km	63	90	11	61

are a) the Southern Ocean where dynamic changes lead to a drop in sea level that is counteracted by positive contributions from glacier mass loss in the northern hemisphere as well as the global sea level rise and b) the high Arctic where the opposite is true: the sea level drop close to glaciated areas in the Arctic (Greenland, Svalbard, Russian Arctic) is counteracted by a sea level rise due to changes in steric and dynamic sea surface height.

4. Discussion and Conclusion

We have analyzed how the time of emergence of an externally forced signal is affected by reducing the background noise through spatial averaging and/or by adding a contribution, namely glacier mass loss, with a high signal-to-noise ratio. Thus, we considered the two largest contributors to global mean sea level rise in the historical period: thermosteric expansion and melting glaciers (Church *et al* 2013).

On regional scales, it is the steric and dynamic sea surface height that dominates the background noise. As roughly 90% of the mass stored in glaciers (excluding Antarctic glaciers) is located north of 60°N, unforced changes in glacier mass are not significant in the ocean areas south of this latitude. Close to glaciated regions around the Arctic Ocean the contribution is stronger but still small compared to the steric and dynamic contribution. With respect to forced trends the situation is different: glaciers have been contributing to sea level rise continuously since 1850 (Gregory *et al* 2013, Marzeion *et al* 2014a, e.g.) leading to a large signal-to-noise ratio of this contribution. The result is an earlier detection away from glaciated regions by about 10 years. Close to the glaciers around the Arctic Ocean the glacier mass loss and concurrent reduction in gravitational attraction leads to a sea level drop that counteracts the rise due to thermal expansion and therefore delays detection.

The spatially inhomogeneous impact of changing glaciers on the potential for detection becomes clear when looking at zonal averages (e.g. figure 1): poleward of 50 °N the signal-to-noise enhancing effect is gradually reduced and even reversed. Apart from that, the glacier contribution hardly contributes to the meridional variability of trends in zonally averaged sea level. The local maximum just north of 45 °S in South Atlantic trends in figure 1 is related to the poleward expansion of the subtropical gyre and the poleward shift of the northern boundary of the Antarctic Circumpolar Current (ACC) under a changing climate (Saenko *et al* 2005, Meijers *et al* 2012, e.g.). The northern boundary of the ACC is related to a strong meridional sea level gradient and transient changes in it's position are accompanied by sea level changes (Yin *et al* 2010, Yin 2012). Such shifts of large scale oceanic features will also change the spatial pattern of internal variability and have to be taken into account when assessing future trends in sea level.

As expected, spatial averaging reduces the background noise from internal variability significantly (figure 3), but not the magnitude of the externally forced signal. This leads to an earlier detection compared to no smoothing (figure 4). With respect to the periods of observations it is useful to know the amount of averaging that is necessary to detect an

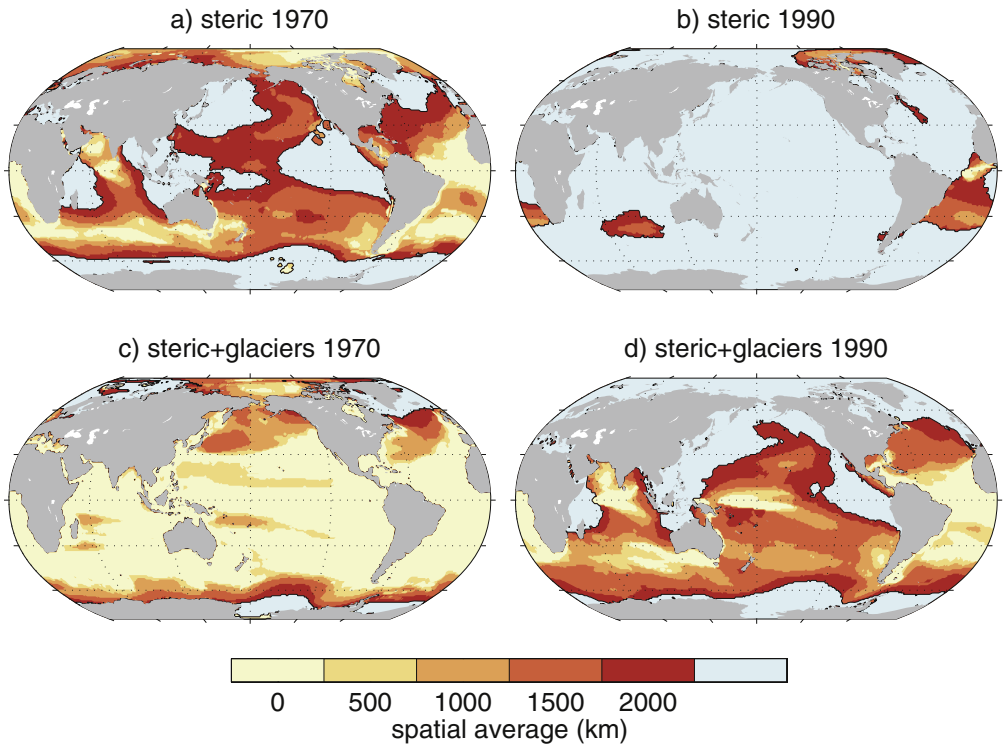

Figure 6. Amount of smoothing that is necessary in order to detect an externally forced signal by 2015 in steric sea surface height (upper row) and the combination of steric height and glacier mass loss (lower row). Two starting years are considered, namely 1970 (left) and 1990 (right). Emergence at e.g. 1000 km means that a signal did emerge at 1000 km but did not at 500 km. It, however, may or may not emerge at 600 km which was not tested. Blue shading indicates that none of the tested spatial filtering resulted in an emergence by 2015.

externally forced signal by 2015 (the recent present). Therefore, we determined the minimum averaging radius at each grid point to achieve detection in 2015 (figure 6). For the steric component extensive averaging is necessary, even on the longer time scale, to detect an externally forced signal. For the past 25 yrs even extensive averaging only leads to a detection in 11% of the ocean area, while an externally forced signal may be detected in 63% of the ocean area during the past 45 yrs (table 1) using large scale averaging in the Pacific and North Atlantic Ocean. This fraction is significantly enhanced (61% and 90%, respectively) when including the glacier contribution.

In this study, we chose to investigate the effect of pre-defined smoothing techniques on the signal-to-noise ratio in linear trends of regional sea level. For individual regions, filters based on physical processes, such as the wind-driven redistribution of ocean volume, may be more efficient by exploiting the compensating variability between regions. Thompson and Merrifield (2014) defined basin-scale ocean regions based on sea level covariance (their figure 1(*a*)) and interestingly, the blue shaded regions in figure 6(*a*) are all located within distinct regions as identified by Thompson and Merrifield (2014). That is, regional averaging within these regions does not reduce the internal variability sufficiently to allow for the emergence of an external signal by 2015. In regions where large scale climate modes govern the sea level variability such as in the Pacific Ocean (Zhang and Church 2012, Hamlington *et al* 2014, e.g.), zonal averaging will be necessary to detect an external signal while in regions more affected by local winds such as the North Sea (Marcos *et al* 2016), averaging over a relatively small area will reduce the noise sufficiently.

During the past decades, the contribution from the Greenland and Antarctic ice sheets to sea level rise has increased and approached the magnitude of the glaciers contribution (Shepherd *et al* 2012, Church *et al* 2013). Estimates of ice sheet mass changes due to internal variability are still poorly constrained but it is likely that recent changes in surface mass balance are partly forced (Bindoff *et al* 2013). Through gravitational adjustments, the bulk of the melted ice will distribute relatively evenly in the tropical and subtropical ocean regions (Mitrovica *et al* 2001). We therefore expect mass loss from ice sheets to lead to a reduction in time of emergence similar to the reduction due to glaciers. However, in the Southern Ocean close to the Antarctic ice sheet, the sea level decrease due to gravitational adjustment will oppose the increase due to thermal expansion (which is small) and glaciers. Depending on the magnitude of the mass loss, this might lead to an earlier detection of a sea level fall close to the regions of greatest mass loss (Lyu *et al* 2014). This is also true close to the Greenland ice sheet. The sea level fall due to the combined mass loss from glaciers and the ice sheet could potentially outpace the sea level rise from thermal expansion and lead to a reduction in time of emergence of a forced signal.

We demonstrated that spatial averaging increases the signal to noise ratio of a forced signal significantly thus increasing the chances of detection within the periods of good observational coverage. However, even with extensive averaging, detection is still not possible in significant parts of the oceans, in particular for the steric and dynamic signal. This does not mean that attempts of detection and attribution are futile but underscores the importance of identifying modes of internal variability accurately to be able to take them into account properly. If this is not possible, spatial averaging offers an alternative tool.

Lastly, the results of this study also highlight the importance of high-quality observations of all the factors contribution to sea level changes. This is particularly important in regions that are subject to the opposing effects of thermal expansion and land ice mass loss such as the northern North Atlantic. While there is a distinct signal in each of these contributors individually, the combined signal may not be distinguishable from the background noise.

Acknowledgments

This work was funded by the Austrian Science Fund (FP253620) and supported by the Austrian Ministry of Science BMWF as part of the UniInfrastrukturprogramm of the Focal Point Scientific Computing at the University of Innsbruck. We acknowledge the World Climate Research Programme's Working Group on Coupled Modelling, which is responsible for CMIP5, and we thank the climate modeling groups (listed in table S1 of this paper) for producing and making available their model output. Two reviewers provided useful comments that helped to improve the publication.

References

Arendt A *et al* 2015 Randolph Glacier Inventory—A Dataset of Global Glacier Outlines: Version 5.0 *Technical report* Global Land Ice Measurements from Space, Boulder Colorado, USA, Digital Media

Bindoff N *et al* 2013 *Detection and Attribution of Climate Change: from Global to Regional* (Cambridge, United Kingdom: Cambridge University Press) section 10, pp 867–952

Church J *et al* 2013 *Sea Level Change* (Cambridge, United Kingdom: Cambridge University Press) section 13, pp 1137–216

Dangendorf S, Marcos M, Müller A, Zorita E, Riva R, Berk K and Jensen J 2015 Detecting anthropogenic footprints in sea level rise *Nat. Comm.* **6** 7849

Domingues C M, Church J A, White N J, Gleckler P J, Wijffels S E, Barker P M and Dunn J R 2008 Improved estimates of upper-ocean warming and multi-decadal sea-level rise *Nature* **453** 1090–3

Dziewonski A and Anderson D 1981 Preliminary reference Earth model *Phys. Earth Planet. In.* **25** 297–356

Farrell W and Clark J 1976 On postglacial sea level *Geophys. J.R. Astron. Soc.* **46** 647–67

Gregory J *et al* 2013 Twentieth-century global-mean sea-level rise: is the whole greater than the sum of the parts? *J. Climate* **26** 4476–99

Hamlington B, Strassburg M, Leben R, Han W, Nerem R and Kim K 2014 Uncovering an anthropogenic sea-level rise signal in the Pacific Ocean *Nat. Clim. Change* **4** 782–5

Hinkel J, Lincke D, Vafeidis A T, Perrette M, Nicholls R J, Tol R S, Marzeion B, Fettweis X, Ionescu C and Levermann A 2014 Coastal flood damage and adaptation costs under 21st century sea-level rise *Proc. Natl Acad. Sci. USA* **111** 3292–7

Lyu K, Zhang X, Church J A, Slangen A B and Hu J 2014 Time of emergence for regional sea-level change *Nat. Clim. Change* **4** 1006–10

Marcos M and Amores A 2014 Quantifying anthropogenic and natural contributions to thermosteric sea level rise *Geophys. Res. Lett.* **41** 2502–7

Marcos M, Marzeion B, Dangendorf S, Slangen A B, Palanisamy H and Fenoglio-Marc L 2016 Internal variability versus anthropogenic forcing on sea level and its components *Surv. Geophys.* **38** 329

Marzeion B, Cogley J G, Richter K and Parkes D 2014b Attribution of global glacier mass loss to anthropogenic and natural causes *Science* **345** 919–21

Marzeion B, Jarosch A H and Gregory J M 2014a Feedbacks and mechanisms affecting the global sensitivity of glaciers to climate change *The Cryosphere* **8** 59–71

Marzeion B, Jarosch A H and Hofer M 2012 Past and future sea-level change from the surface mass balance of glaciers *The Cryosphere* **6** 1295–322

Marzeion B and Levermann A 2014 Loss of cultural world heritage and currently inhabited places to sea-level rise *Environ. Res. Lett.* **9** 034001

Meijers A, Shuckburgh E, Bruneau N, Sallee J B, Bracegirdle T and Wang Z 2012 Representation of the Antarctic Circumpolar Current in the CMIP5 climate models and future changes under warming scenarios *J. Geophy. Res.: Oceans* **117** C12008

Meyssignac B, Salas y, Melia D, Becker M, Llovel W and Cazenave A 2012 Tropical Pacific spatial trend patterns in observed sea level: internal variability and/or anthropogenic signature? *Climate of the Past* **8** 787–802

Milne G and Mitrovica J 1998 Postglacial sea-level change on a rotating Earth *Geophys. J. Int.* **133** 1–19

Mitrovica J X, Tamisiea M E, Davis J L and Milne G A 2001 Recent mass balance of polar ice sheets inferred from patterns of global sea-level change *Nature* **409** 1026–9

Myhre G *et al* 2013 *Anthropogenic and Natural Radiative Forcing* (Cambridge, United Kingdom: Cambridge University Press) section 8, pp 659–740

Richter K and Marzeion B 2014 Earliest local emergence of forced dynamic and steric sea-level trends in climate models *Environ. Res. Lett.* **9** 114009

Saenko O A, Fyfe J C and England M H 2005 On the response of the oceanic wind-driven circulation to atmospheric CO_2 increase *Clim. Dyn.* **25** 415–26

Shepherd A *et al* 2012 A reconciled estimate of ice-sheet mass balance *Science* **338** 1183–9

Slangen A B, Church J A, Agosta C, Fettweis X, Marzeion B and Richter K 2016 Anthropogenic forcing dominates global mean sea-level rise since 1970 *Nat. Clim. Change* **6** 701–5

Slangen A B, Church J A, Zhang X and Monselesan D 2014b Detection and attribution of global mean thermosteric sea level change *Geophys. Res. Lett.* **41** 5951–9

Taylor K, Stouffer R and Meehl G 2012 An overview of CMIP5 and the experiment design *Bull. Am. Meteorol. Soc.* **93** 485–98

Thompson P. R and Merrifield M. A 2014 A unique asymmetry in the pattern of recent sea level change *Geophys. Res. Lett.* **41** 7675–83

Van Vuuren D *et al* 2011 The representative concentration pathways: an overview *Clim. Change* **109** 5–31

Yin J 2012 Century to multi-century sea level rise projections from CMIP5 models *Geophys. Res. Lett.* **39** L17709

Yin J J, Griffies S M and Stouffer R J 2010 Spatial variability of sea level rise in twenty-first century projections *J. Clim.* **23** 4585–607

Zhang X and Church J A 2012 Sea level trends, interannual and decadal variability in the Pacific Ocean *Geophys. Res. Lett.* **39** L21701